The influence of capping layers on pore formation in Ge during ion implantation

H. S. Alkhaldi, Tuan T. Tran, F. Kremer, and J. S. Williams

Citation: Journal of Applied Physics **120**, 215706 (2016); doi: 10.1063/1.4969051
View online: http://dx.doi.org/10.1063/1.4969051
View Table of Contents: http://aip.scitation.org/toc/jap/120/21
Published by the American Institute of Physics

Articles you may be interested in

Migration processes of the As interstitial in GaAs
Journal of Applied Physics **120**, 215705215705 (2016); 10.1063/1.4969049

JOURNAL OF APPLIED PHYSICS **120**, 215706 (2016)

The influence of capping layers on pore formation in Ge during ion implantation

H. S. Alkhaldi,[1,2] Tuan T. Tran,[1] F. Kremer,[3] and J. S. Williams[1]
[1]*Department of Electronic Materials Engineering, Research School of Physics and Engineering, The Australian National University, Canberra, Australian Capital Territory 2601, Australia*
[2]*Department of Physics, College of Education—Jubail, Dammam University, Dammam 1982, Saudi Arabia*
[3]*Centre for Advanced Microscopy, The Australian National University, Australian Capital Territory 2601, Australia*

(Received 2 August 2016; accepted 15 November 2016; published online 2 December 2016)

Ion induced porosity in Ge has been investigated with and without a cap layer for two ion species, Ge and Sn, with respect to ion fluence and temperature. Results without a cap are consistent with a previous work in terms of an observed ion fluence and temperature dependence of porosity, but with a clear ion species effect where heavier Sn ions induce porosity at lower temperature (and fluence) than Ge. The effect of a cap layer is to suppress porosity for both Sn and Ge at lower temperatures but in different temperatures and fluence regimes. At room temperature, a cap does not suppress porosity and results in a more organised pore structure under conditions where sputtering of the underlying Ge does not occur. Finally, we observed an interesting effect in which a barrier layer of a-Ge that is denuded of pores formed directly below the cap layer. The thickness of this layer (~ 8 nm) is largely independent of ion species, fluence, temperature, and cap material, and we suggest that this is due to viscous flow of a-Ge under ion irradiation and wetting of the cap layer to minimize the interfacial free energy. *Published by AIP Publishing.*
[http://dx.doi.org/10.1063/1.4969051]

I. INTRODUCTION

Germanium (Ge) has become an increasingly important material for a range of applications in microelectronic devices[1] due to higher carrier mobility and smaller bandgap than silicon (Si). Doping Ge with high Sn concentration has also opened up applications for Ge-Sn photonics.[2] However, in all such applications that rely on ion implantation doping of Ge, the formation of a porous layer on the Ge surface is a significant issue and must be avoided or minimized.[3] For example, the formation of porosity in Ge has been reported to occur during ion implantation of crystalline Ge at room temperature (RT) at quite moderate implant fluences. It results in significant surface morphology associated with volumetric swelling and the formation of amorphous porous layers.[4–6] This affect has been observed for a wide range of heavy ions at keV energies and occurs at a threshold fluence of around 10^{15} ions/cm^2.[7–9] Although deleterious for many microelectronic applications, such nanoporous structures with nm scale can have wide applications including in lithium ion batteries as an anode,[10] in gas sensors,[11] in thermoelectric applications,[12] and even in specific optoelectronic applications.[13] Most of the previous studies on porosity in irradiated Ge have focused on the evolution and understanding of porous structures quantitatively and qualitatively. Up to now, few studies have focused on studying the suppression of a porous structure. Generally, based on literature reports, porosity is often suppressed at liquid nitrogen implantation temperature (LN_2T) for most heavy ion implant species. Holland *et al.*[14] found that implanting Bi^+ into Ge at LN_2T could suppress the pore formation at fluences up to 4×10^{15} ions/cm^2. Stritzker *et al.*[5] also observed that a porous structure was eliminated at LN_2T for self-ion implantation of Ge even at high fluences up to 1×10^{17} ions/cm^2. Our previous results[15] support this latter conclusion for self-ion irradiation of both Ge substrates and $Si_{1-x}Ge_x$ alloys even at fluences higher than 1×10^{17} ions/cm^2. However, for some ion species, porous structures or surface microstructural features have been observed in Ge even at LN_2T. For example, Holland *et al.*[14] detected blackening on the surface at a fluence of 3×10^{16} ions/cm^2 when implanting with 120 keV Sn^+ ions, which is indicative of structural changes in Ge, but they did not show any TEM images of the microstructure. Similarly, recent work by Tran *et al.*[2] observed porous structures by implanting 100 keV Sn^+ ions with fluences between 2.5×10^{16} and 5×10^{16} ions/cm^2 for Sn^+ at LN_2T. This is consistent with the finding of Bruno *et al.*,[16] who observed a honeycomb-like structure for antimony (Sb) implanted Ge at LN_2T to a fluence of 6.4×10^{15} ions/cm^2 at 50 keV. Clearly, these reports show that for some heavy ion species, LN_2T bombardment does not suppress porosity.

In terms of capping the Ge surface prior to implantation, as a possible means of suppressing porosity, there have been few previous studies. Appleton *et al.*[8] revealed that the free surface of Ge is not necessary for initial void nucleation after coating the surface with an aluminum (Al) film of ~80 nm and then implanting 230 keV Ge^+ at RT with a fluence of 2×10^{16} ions/cm^2. They observed that a porous structure still formed underneath the cap layer and concluded that the initial crater formation is not a sputtering process as suggested by Wilson,[4] but relates to vacancy agglomeration at the Ge surface under a cap. In addition, Janssens *et al.*[17] also deposited a thin SiO_2 film on the surface prior to implantation at

RT with Sb, arsenic (As), and gallium (Ga) ions at keV energies. At fluences between 1×10^{15} and 3×10^{15} ions/cm^2, they found that subsurface void formation and porosity cannot be suppressed for Sb ions by using a cap layer, but no porous structure was observed for As and Ga ions, although it is unclear whether porosity occurred for Ga and As ions without a cap. They also suggested that voids form as a result of vacancy clustering, not sputtering, and thus, the Ge expands beneath the oxide layer. Although not specifically examining a cap layer on Ge for suppression of porosity, Darby *et al.*[18,19] examined the effect of deposited Ge layers on both Ge and SiO_2. They found that depositing an evaporated Ge film onto thermally grown layers of SiO_2 results in the formation of a normal columnar (porous) structure, whereas in sputtered Ge films voids develop and expand isotropically. The specific location of the nucleation sites for pore formation in such deposited films is likely to cause this change in morphology. It is noteworthy that, in both sputtered and evaporated films, a continuous a-Ge layer of ~8 nm thickness on top of the porous structure was found to be devoid of pores.

In contrast to these previous RT studies with a capping layer, where porosity was still observed, Tran *et al.*[2] found that a capping layer of 20 nm thick SiO_2 prior to implantation at LN_2T with Sn^+ ions completely suppressed the porous structure. Presumably, the different implant temperature is responsible for this favorable result, which is thought to be a result of low mobility of point defects in this low temperature regime, combined with the behavior of a cap layer as an obstacle for vacancy clustering, thus preventing the pore formation.[2]

In the current study, we have focused on examining the effect of a cap layer on pore formation with respect to ion fluence, temperature, thickness of the cap layer, and ion species. We found that a cap layer can suppress porosity in Ge in some cases, depending on the irradiation temperature and ion mass. In addition, even when a porous structure develops, there is a continuous a-Ge layer of ~8 nm thickness immediately under the cap that is denuded of pores, and we discuss this in terms of a wetting phenomenon of the a-Ge due to its viscous flow under the cap.

II. EXPERIMENTAL METHODS

Undoped crystalline Ge wafers of (100) orientation were used as substrates. Various capping layers of SiO_2, Al, and amorphous Si (a-Si) were used prior to ion bombardment. A SiO_2 cap layer was deposited onto selected Ge samples with thicknesses of 20 nm and 40 nm. The deposition of both the SiO_2 and a-Si cap layers was carried out using plasma enhanced chemical vapour deposition (PECVD). The deposition rate was 58 nm/min at a temperature of 300 °C. For an Al cap layer, we used an e-beam evaporator. The thickness of a-Si and Al cap layers was 40 nm.

All the above Ge and SiO_2 capped samples were then implanted with 140 keV Ge^- ions and 225 keV Sn^+ ions at the ANU Heavy Ion Accelerator Facility. For Al and a-Si capped samples, 140 keV Ge^- ions were implanted at RT. To minimise channelling effects, the sample holder was misoriented by 7° to the normal beam direction and ion fluences up to 2×10^{16} ions/cm^2 were used. The sample holder temperatures varied between −180 °C and 100 °C and were held constant during irradiation with a deviation of ±3 °C, achieved by connecting a CrAl thermocouple to the sample holder. The average ion flux for Ge ions and Sn ions was $\sim 1.2 \times 10^{13}$ ions/cm^2/s and 6.9×10^{11} ions/cm^2/s, respectively. Part of the sample was masked using a Si wafer to provide a well-defined edge between the irradiated and the non-irradiated areas.

According to SRIM simulation,[20] the projected ion range, the longitudinal straggling, the energy loss (nuclear and electronic), the sputtering yield, and the maximum production depth for vacancies under the irradiation conditions are summarized in Table I. Compared with nuclear energy loss, the electronic energy loss is negligible at the implantation energies, which were chosen to obtain a similar projected range R_p for both Ge and Sn ions.

A Dektak stylus profilometer was used to determine the step height between the unimplanted and the implanted regions. A plan-view of the sample surface was obtained using plan-view scanning electron microscopy (PVSEM) with a Zeiss-UltraPlus field effect (FE) SEM. The structure underneath the surface was observed by cross-sectional transmission electron microscopy (XTEM), which was performed with a Philips CM300 microscope operating at 300 keV. An elemental concentration map under the capping layer was investigated by using energy dispersive x-ray (EDX) analysis with a JEOL 2100 F instrument.

III. RESULTS

In Fig. 1, we illustrate by XTEM typical behaviour of Ge bombarded with Ge^- and Sn^+ ions at LN_2T, including the use of a SiO_2 cap prior to Sn ion bombardment. Self-ion implantation of Ge at LN_2T, even for fluences up to 1×10^{17} ions/cm^2, produces a thick a-Ge layer but no pore formation was observed as shown in Fig. 1(a). In contrast, similar to the work of Tran *et al.*,[2] LN_2T does not suppress the porous structure when implanting Sn with a lower fluence of 3×10^{16} ions/cm^2, as can be seen in Fig. 1(b). In this case, the top 2/3rd of the a-Ge layer contains large columnar pores that intersect the surface, consistent with

TABLE I. Projected ion Range R_p, longitudinal straggling ΔR_p, Nuclear energy loss $(dE/dx)_{nucl}$, electronic energy loss $(dE/dx)_{el}$, maximum vacancy production depth, and sputtering yield for 140 keV Ge^+ and 225 keV Sn^+ implanted into Ge, from SRIM simulations.[25]

Target	Energy (keV)	Ion species	R_p (nm)	ΔR_p (nm)	$(dE/dx)_{el}$ (keV/nm)	$(dE/dx)_{nucl}$ (keV/nm)	Maximum vacancy production depth (nm)	Sputtering yield atom/ion
Ge	140	Ge	62.2	30.1	0.2	1.5	27.2	4.2
Ge	225	Sn	65.1	25.8	0.2	2.8	32.7	5.7

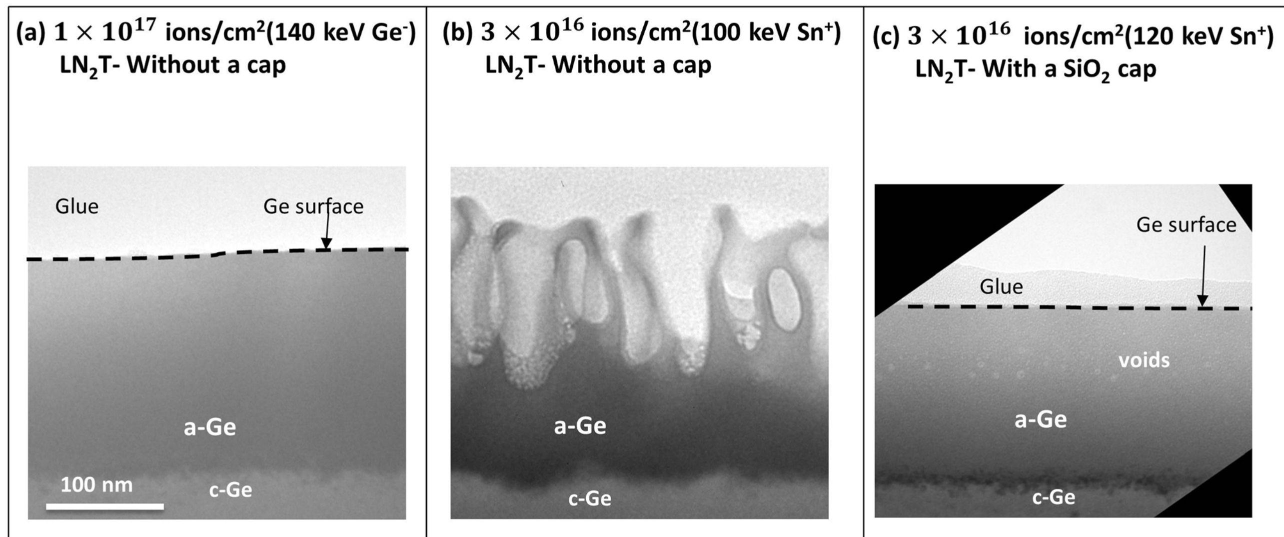

FIG. 1. XTEM images of Ge implanted with Sn and Ge ions at LN_2T with and without a SiO_2 cap layer. (a) 1×10^{17} ions/cm^2 with 140 keV Ge^- ions without a cap layer; (b) 3×10^{16} ions/cm^2 100 keV Sn^+ ions without a cap; (c) 3×10^{16} ions/cm^2 120 keV Sn^+ ions with a SiO_2 cap layer; in (c), the cap layer has been removed prior to the XTEM analysis. The scale bar is the same for all XTEM images.

typical porosity microstructure in irradiated Ge.[14,15] In contrast, capping the surface with a SiO_2 layer of 20 nm thickness totally eliminated pore formation at LN_2T at the same Sn fluence as shown in Fig. 1(c). The implant energy of the Sn ions was slightly higher to account for energy loss due to penetration through the cap layer. However, a band of small voids is observed in the a-Ge layer, close to the depth of maximum energy deposition. As discussed previously,[2] this band presumably arises from agglomeration of vacancies at the depth of maximum vacancy production rather than vacancy migration to the surface, where clustering and void formation appear to nucleate pores in the uncapped case. Comparing the Ge and Sn behaviours at LN_2T, for uncapped samples, the heavier Sn ions cause pores to form, whereas Ge ions do not. The understanding of this behaviour in terms of the effect of higher nuclear energy loss and/or chemical effects in case of Sn is treated in Sec. IV. Indeed, differences between the porous behaviour of the two ion species and the effect of a cap on the data of Fig. 1 were the motivations for the current study.

A. Ion fluence dependence

Figs. 2(a)–2(l) show PVSEM and XTEM micrographs following self-ion implantation of Ge with 140 keV ions at RT with and without a cap layer of SiO_2 at different fluences.

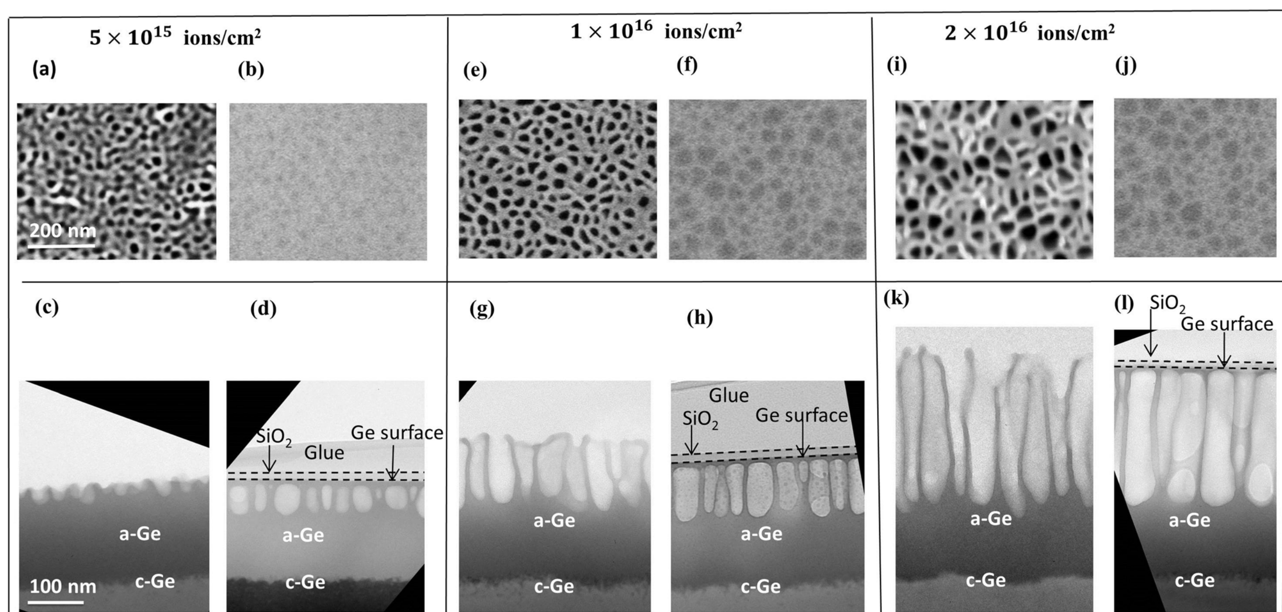

FIG. 2. PVSEM and XTEM images for different ion fluences for self-ion implantation of Ge with 140 keV implanted at RT with a cap layer of SiO_2 and without a cap layer; (a) and (c) 5×10^{15} ions/cm^2 without a cap; (b) and (d) 5×10^{15} ions/cm^2 with 20 nm of a SiO_2 layer; (e) and (g) 1×10^{16} ions/cm^2 without a cap layer; (f) and (h) 1×10^{16} ions/cm^2 with a cap layer; (i) and (k) 2×10^{16} ions/cm^2 without a cap layer; (j) and (l) 2×10^{16} ions/cm^2 with a cap layer; in (l), the cap layer partly has been removed due to sputtering. The scale bars in (a) and (c) are the same for all PVSEM and XTEM images, respectively.

The evolution of the pore structure with fluence at RT with no cap is consistent with our previous results. For example, the pore structure appears to nucleate from voids at the surface at low fluence (Fig. 2(c)) and then extends as columns with thin walls as the fluence increases (Figs. 2(g) and 2(h)). The pore size increases slowly from 10 to 16 nm for fluences from 5×10^{15} to 2×10^{16} ions/cm^2 (Figs. 2(a), 2(e), and 2(i)). From the XTEM images in Fig. 2, it is clear that a porous structure in Ge both with a cap layer and without a cap layer forms in a-Ge at RT, consistent with prior understanding.[15,17]

For the capped samples, the evolution of a porous structure at RT, in terms of near surface void nucleation and development of a columnar structure, is essentially similar to uncapped samples. However, in all of the capped samples, there is a band of a-Ge immediately under the cap that is denuded of pores and is approximately 8 nm in thickness. This band suggests that vacancy agglomeration and pore formation are suppressed immediately below the cap layer, but it is surprising that this denuded layer does not change in thickness with fluence. Looking further at the detailed differences between capped and uncapped samples, it appears that at the low fluence of 5×10^{15} ions/cm^2 (see Fig. 2(d)), the cap layer may actually contribute to an ordered porous structure once porosity develops, with larger voids apparent in the capped sample, but the voids do not extend to the surface. Furthermore, the porous structure for samples with a capping layer seems to be relatively uniform and well-ordered, with the individual pores more homogeneous in appearance and having walls that are mostly more vertical compared with the cases without the cap layer for almost all fluences (see Figs. 2(d), 2(h), and 2(i)). Presumably, sputtering of the porous layer at the a-Ge surface in uncapped samples contributes to the observed less ordered columnar arrangement in such cases. In summary, when the cap layer is present prior to implantation, the porous structure still forms at RT, but there is a non-porous a-Ge barrier layer directly underneath the cap layer.

The fluence dependence of pore formation with Sn ions at RT, with and without a cap, is shown by the PVSEM and XTEM images in Figs. 3(a)–3(l). Basically, the pore evolution with Sn ion fluence is essentially similar to the case of Ge ions. It is interesting that the barrier layer denuded of pores is again around 8 nm in thickness, despite the heavier Sn ions and higher rate of nuclear energy deposition under the cap. Significant difference between Sn and Ge is that pore nucleation occurs at a lower ion fluence for heavier Sn ions. In addition, some patchy surface structures for the capped Sn implanted Ge samples at the two highest fluences are observed. We consider that this is due to effective sputter removal of portions of the 20 nm cap at such fluences, noting that a Sn fluence of 5×10^{16} ions/cm^2 totally removes the cap.[2]

Figs. 4(a) and 4(b) show volumetric swelling as a function of implanted ion fluence with a SiO_2 cap layer of 20 nm thickness and without a cap layer. Fig. 4(a) shows self-ion implantation of Ge irradiated at 140 keV, and Fig. 4(b) is for Sn ions irradiated at 225 keV. The data show swelling which increases with ion fluence for both ion species, and slightly less swelling for samples implanted with the cap layer. By comparing the step height in Sn to the one in Ge, it is clear that the volumetric expansion in Sn (∼210 nm) is much

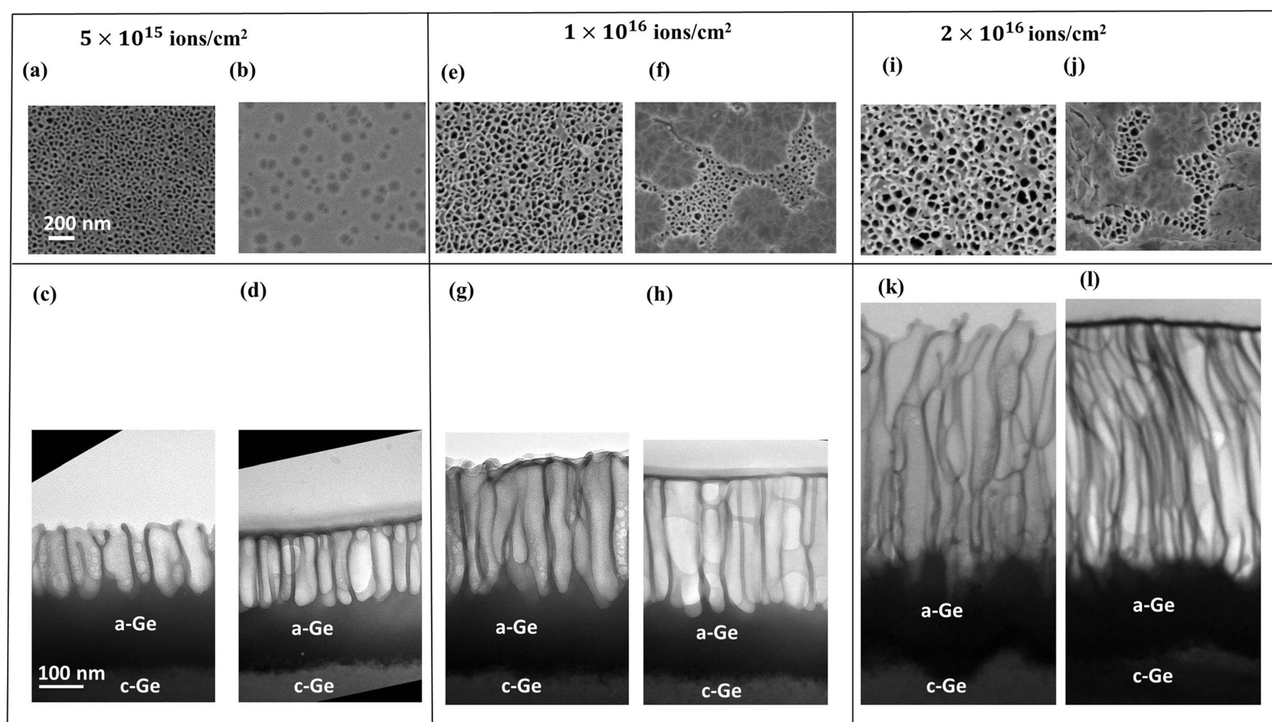

FIG. 3. PVSEM and XTEM images for different ion fluences for implanting Ge with 225 keV Sn^+ at RT with a 20 nm SiO_2 cap layer and without a cap layer; (a) and (c) 5×10^{15} ions/cm^2 without a cap layer; (b) and (d) 5×10^{15} ions/cm^2 with a cap layer; (e) and (g) 1×10^{16} ions/cm^2 without a cap layer; (f) and (h) 1×10^{16} ions/cm^2 with a cap layer; (i) and (k) 2×10^{16} ions/cm^2 without a cap layer; (j) and (l) 2×10^{16} ions/cm^2 with a cap layer; in (l), the cap layer has been removed due to sputtering. The scale bars are the same in (a) and (c) for all PVSEM and XTEM images, respectively.

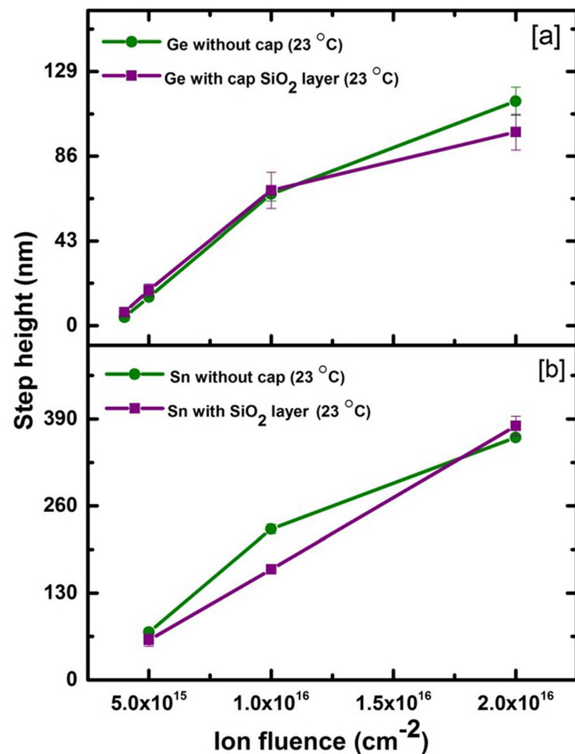

FIG. 4. Step height due to volumetric swelling as a function of implanted fluence in Ge implanted with 140 keV Ge⁻ ions at RT with and without a 20 nm SiO_2 layer (a); and Ge implanted with 225 keV Sn^+ ions at RT with and without a 20 nm SiO_2 layer (b).

larger than in Ge (∼120 nm) at an implanted fluence of 2×10^{16} ions/cm^2. This effect may be due to the slightly higher projected ion range of Sn and the higher nuclear energy deposition which results in a thicker a-Ge layer (see Table I).

B. Temperature dependence of porosity

In this section, we highlight the effect of temperature on the pore formation with and without a SiO_2 cap layer. One fluence has been selected (2×10^{16} ions/cm^2), with one thickness of cap layer (20 nm).

Figs. 5(a)–5(h) show PVSEM and XTEM images for self-ion implantation of Ge at LN_2T and −50 °C, with and without a SiO_2 cap layer of 20 nm thickness. It is obvious that irradiation at LN_2T suppresses the porous structure regardless of the presence of a cap layer. This is consistent with the result in Fig. 1(a) at a much higher Ge$^-$ ion fluence. However, implanting at −50 °C without a cap layer develops a clear porous layer with a well-defined columnar structure with a thickness of 153 nm (see Figs. 5(e) and 5(g)) overlaying an a-Ge layer of similar thickness. In contrast, with a cap at −50 °C there is clear suppression of a pore layer: the a-Ge is largely intact with occasional large voids under the cap as shown in Figs. 5(f) and 5(h).

In the case of Sn ions, Fig. 6 shows that no obvious porous structure is observed for both capped and uncapped samples under LN_2T at a fluence of 2×10^{16} ions/cm^2. We note that

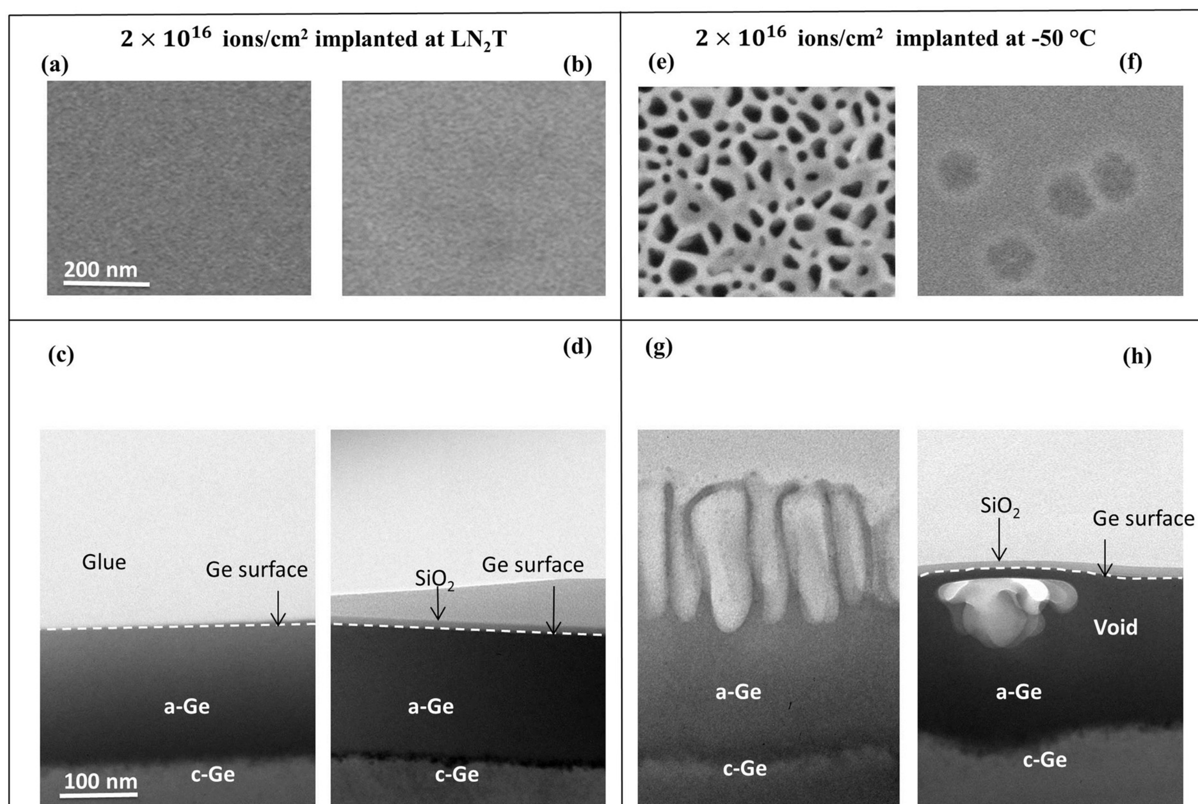

FIG. 5. PVSEM and XTEM images for Ge implanted with 140 keV Ge⁻ ions under different temperatures with a 20 nm SiO_2 cap and without a cap layer; (a) and (c) 2×10^{16} ions/cm^2 at LN_2T without a cap; (b) and (d) 2×10^{16} ions/cm^2 at LN_2T with a cap layer;. (e) and (g) 2×10^{16} ions/cm^2 at −50 °C without a cap layer; (f) and (h) 2×10^{16} ions/cm^2 at −50 °C with a cap layer. The scale bars in (a) and (c) are the same for all PVSEM and XTEM images, respectively.

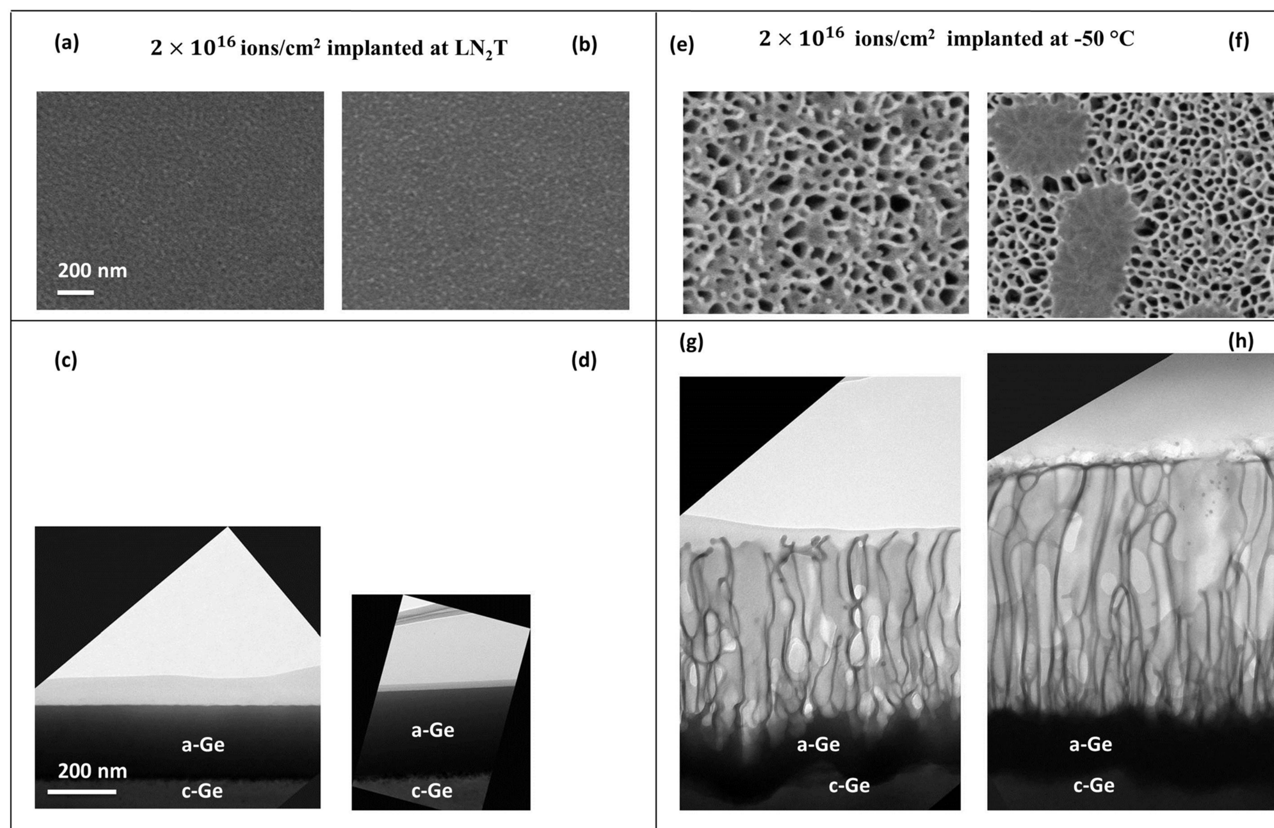

FIG. 6. PVSEM and XTEM images for Ge implanted with 225 keV Sn^+ ions at different temperatures with a 20 nm cap layer of SiO_2 and without a cap layer; (a) and (c) 2×10^{16} ions/cm^2 at LN_2T without a cap; (b) and (d) 2×10^{16} ions/cm^2 at LN_2T with a cap layer; (e) and (g) 2×10^{16} ions/cm^2 at $-50\,°C$ without a cap; (f) and (h) 2×10^{16} ions/cm^2 at $-50\,°C$ with a cap layer; in (h), the cap layer has been removed due to sputtering. The scale bars in (a) and (c) are the same for all PVSEM and XTEM images, respectively.

this fluence is just below the threshold fluence for pore formation with Sn ions since a fluence of 3×10^{16} ions/cm^2 gives rise to a clear porous structure as shown in Fig. 1(b) for the case without a SiO_2 cap.

However, as the temperature is increased to $-50\,°C$, both capped and uncapped samples show the formation of a porous structure (see Figs. 6(e)–6(h)), indicating that, at this ion fluence (2×10^{16} ions/cm^2), the formation of a porous structure is not suppressed at $-50\,°C$, regardless of the use of a cap layer. We note that at a lower Sn ion fluence of 5×10^{15} ions/cm^2 at $-50\,°C$ (not shown), a porous structure does not develop, only isolated large voids similar to the situation for Ge ions at higher fluence in Fig. 5(h). Thus, ion species, fluence, and irradiation temperature influence pore formation in Ge with and without a cap layer.

In summary, there are significant differences between Sn and Ge ions in terms of development of a porous structure in Ge. The first difference is at LN_2T, where a porous structure is always suppressed with Ge ions even at very high fluences with or without a cap layer. However, with Sn ions without a cap layer, a porous structure is not suppressed if the ion fluence is above a threshold fluence which is around 2.5–3×10^{16} ions/cm^2. However, by coating the surface with a SiO_2 film, porosity is suppressed at high Sn ion fluences well above the threshold for porous development without a cap. Second, if the temperature is increased to $-50\,°C$, a porous structure occurs in Ge at a Sn ion fluence of 2×10^{16} ions/cm^2 both with and without a cap, but the situation with Ge ions is quite different. Pore formation fully develops at 2×10^{16} Ge^- ions/cm^2 without a cap, whereas the a-Ge layer is largely intact at this fluence with occasional large voids when a cap layer is used. This suggests that, if the fluence is increased beyond 2×10^{16} ions/cm^2 in this latter case, pore formation may fully develop. Hence, both the ion fluence and the temperature are playing an important role in terms of suppressing or enhancing the development of a porous structure with and without a cap layer, and for heavier ions the onset of porosity occurs at a lower fluence.

Fig. 7 shows the volumetric expansion as a function of implant temperature for irradiation of Ge with both Ge (a) and Sn (b) ions, with and without a cap. In Fig. 7(a), the measured step height is consistent with the TEM results. At LN_2T, with Ge ions the swelling is less than 1 nm consistent with a thick a-Ge layer with no porosity. When the temperature increases to $-50\,°C$, the step height is shown to be 65 nm for the samples without a cap, but only 3.9 nm for the samples with such a cap. This is again consistent with the XTEM results in Fig. 5 where occasional large voids are observed with a cap, whereas a decidedly porous structure occurs without a cap. In the case of Sn in Fig. 7(b), the step height shows no swelling at LN_2T for both capped and uncapped samples, consistent with no porous structure observed in XTEM images. However, implantation at $\geq -50\,°C$ and RT develops a porous structure regardless of a

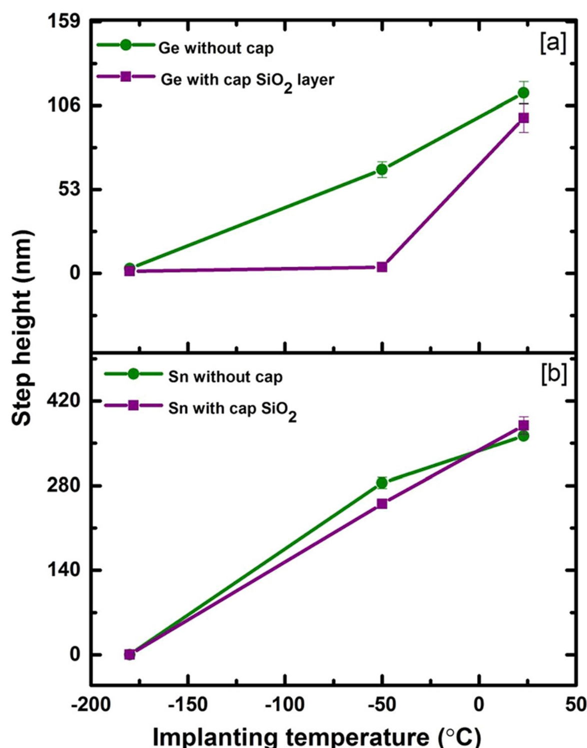

FIG. 7. Volumetric swelling as a function of implantation temperature in Ge for Ge and Sn ions at a fluence of 2×10^{16} ions/cm^2; (a) 140 keV Ge$^-$ ions with and without a cap layer of 20 nm SiO_2; (b) 225 keV Sn^+ ions with and without a cap layer of 20 nm SiO_2.

cap layer and the swelling is essentially the same for cap and no cap cases.

C. The effect of cap layer thickness

To study the effects of cap layer thickness, two thicknesses of the cap layer (20 nm and 40 nm of SiO_2) were deposited onto Ge prior to implantation and a fluence of 1×10^{16} ions/cm^2 was selected at RT for both Ge and Sn ions.

Fig. 8 shows XTEM images for Ge capped with 40 nm of SiO_2 and implanted with both Ge and Sn ions to a fluence of 1×10^{16} ions/cm^2 at RT. These images should be compared with Figs. 2(h) and 3(h) for a 20 nm SiO_2 cap layer. The only significant change observed was a reduction in the porous layer thickness for both Ge and Sn ions for the 40 nm layer compared with the 20 nm layer. The cap layer thickness does not show any significant difference in terms of porous layer formation, pore diameter, and degree of swelling, which is in good agreement with earlier studies of Janssens *et al.* for Sb bombarded Ge.[17] We note that the layer of a-Ge denuded of pores directly under the cap layer remains close to 8 nm thick regardless of the cap thickness.

IV. DISCUSSION

Overall, there are clear trends obtained from this study relating to the formation and evolution of porosity in ion irradiated Ge. The data are consistent with previous studies, where there are clear dependencies on ion fluence and temperature. In terms of ion fluence, there is a threshold fluence above which porosity nucleates and develops in ion

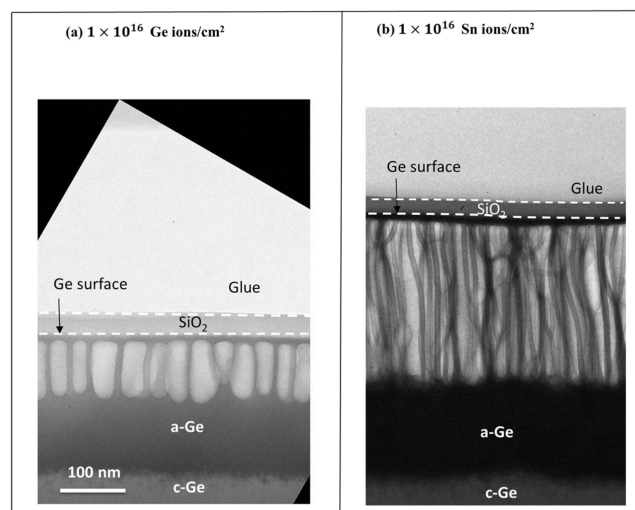

FIG. 8. XTEM images for a selected fluence of 1×10^{16} ions/cm^2 for 40 nm thickness of a cap layer implanted at RT (a) 140 keV Ge$^-$ ions; (b) 225 keV Sn^+ ions. The scale bar is the same for both XTEM images.

amorphized Ge. In addition, for each ion species there appears to be a temperature range in which porosity is favored: below this window, porosity is difficult or impossible to develop even at extremely high ion fluence, and above this window, Ge cannot be rendered amorphous which is a prerequisite for pore formation.[5] We have also observed a significant ion species dependence, whereby the heavier ion Sn clearly promotes pore formation at lower temperatures compared with Ge ions, noting that Ge ion irradiation cannot initiate pores in Ge at any fluence at LN_2T, whereas Sn ion irradiation can initiate porosity at moderate fluences ($>2 \times 10^{16}$ ions/cm^2) at this temperature (Fig. 1). We have insufficient data to establish whether this species effect is caused by the higher nuclear energy deposition of Sn ions (higher density of vacancies produced along ion tracks) or whether chemistry plays a role. For example, does a higher vacancy production rate favor agglomeration of vacancies into voids even at LN_2T or does Sn (when its concentration builds up to several atomic percent) enhance vacancy migration and/or agglomeration via a chemical effect as suggested in our recent publication?[2] Further studies, for example, with a wider range of ion species, would be needed to resolve this issue.

In terms of an SiO_2 capping layer, its effect in retarding porosity is apparent in some cases in the data presented, but the role of the cap in influencing vacancy agglomeration (at the cap-Ge interface for example) appears to be quite complex. Clearly, in the case of both Sn and Ge ions at low temperatures, the presence of a SiO_2 cap suppresses porosity, appearing to substantially increase the threshold fluence for the development of porous layers (at LN_2T for Sn ions and at $-50\,°C$ for Ge ions). This conclusion is supported by the fact that, at the same 3×10^{16} ions/cm^2, fluence at LN_2T Sn ions causes a well-developed porous layer without a cap, whereas only small voids are observed with a cap (Figs. 1(b) and 1(c)). For Ge ions, this behavior appears at a higher temperature ($-50\,°C$) as shown in Figs. 5(g) and 5(h). At RT, where a cap does not significantly suppress porosity (at least under the ion fluence/species conditions in this study), there is actually

evidence that once porosity is initiated, a SiO_2 cap may facilitate its development into an ordered structure (see Figs. 2(c) and 2(d)). Another effect of a cap is that it suppresses sputtering of the underlying Ge layer and this lack of sputtering may contribute to the more ordered porous structure. To help understand why a cap can suppress porosity particularly at low temperature, it is important to review the understanding of the nucleation of pores in a-Ge under ion irradiation. For keV ion irradiation, there is now considerable evidence in the literature that vacancy agglomeration first occurs at the Ge surface (in uncapped samples) rather than at the peak of the nuclear energy deposition density (maximum in vacancy production).[14] Further details of the vacancy clustering mechanism of porous formation and vacancy migration to the surface can be found in Refs. 9, 14, 15, and 21. Indeed, in Fig. 2(c), it is clear that voids develop first at the Ge surface at a low fluence of 5×10^{15} ions/cm^2 at RT. In contrast, when a cap is used, the surface of the Ge in contact with the cap appears denuded of voids and Fig. 1(c) shows that voids nucleate deeper in the a-Ge layer (at least for the LN_2T Sn irradiation case). This may suggest that a cap layer suppresses vacancy agglomeration at the Ge surface, the region where pores nucleate in the uncapped case, thus raising the critical fluence for nucleation of pores. Alternatively, the presence of a mechanically more rigid cap at lower irradiation temperatures may restrict the viscous flow of underlying a-Ge under irradiation and hence inhibit expansion of the a-Ge layer, thus suppressing vacancy agglomeration. We note that the viscous flow of both a-Si[22,23] and a-Ge[23,24] materials has previously been observed under ion irradiation. We explore below both this issue and possible reasons for the lack of void formation in a continuous a-Ge barrier layer directly below a SiO_2 cap layer.

The barrier layer denuded of pores directly under the cap has a constant thickness of ~8 nm regardless of ion fluence, energy, mass, or temperature. Even if the temperature is raised to 100 °C as is shown in Fig. 9, the thickness of the barrier layer does not change significantly. In the literature, there are few data with XTEM images of porosity under a cap layer. Indeed, Appleton *et al.*[8] and Janssens *et al.*[17] reported that pore formation does not extend to the surface when a cap layer is present, but they do not clearly demonstrate a barrier layer under a cap. However, in the work by Darby *et al.*,[18,19] there appears to be a clear pore-free layer with the same thickness as in our case in deposited Ge layers on SiO_2 following ion irradiation. No explanation was given as to the origin of such layers in this case.

What then is the explanation for the formation of such a barrier layer between the cap and a porous subsurface layer? First, this layer could be the result of ion-induced intermixing of Si and O with the underlying Ge layer. To explore such intermixing, Fig. 10(a) shows two EDX spectra of the Si and O distribution in the underlying Ge, indicating significant intermixing of O and Si directly below the cap compared with O and Si concentrations at depths below the porous layer. It could be that significant O (and Si) in a-Ge could inhibit vacancy agglomeration under the cap layer. Indeed, we have previously shown that porosity is suppressed in $Si_{1-x}Ge_x$ alloys as the Si content increases.[15] Janssens *et al.* also found

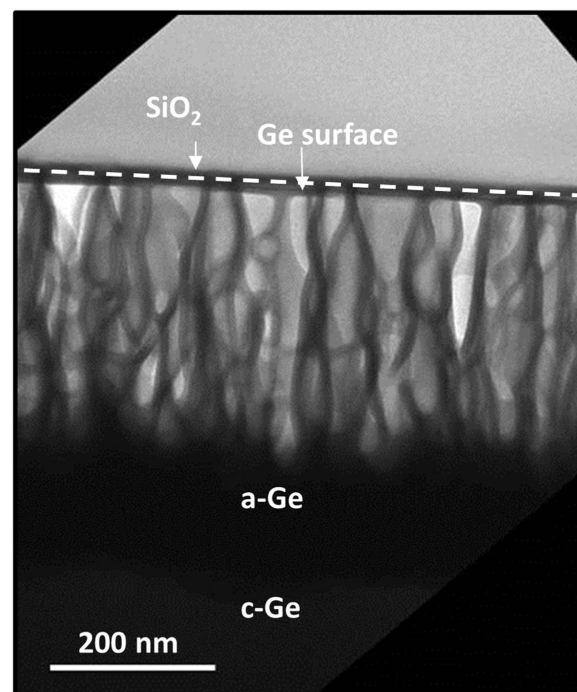

FIG. 9. XTEM images for a fluence of 2×10^{16} ions/cm^2 implanted into Ge with 140 keV Ge$^-$ at 100 °C. The cap layer has been removed due to sputtering.

that subsurface regions contain a large amount of O under a SiO_2 cap.[17] However, we would expect the degree of intermixing and O/Si concentration-depth distributions to be significantly different as a function of ion species (that is, for Ge and heavier Sn ion irradiations) and at different fluences. In contrast, the barrier layer thickness remains constant, independent of ion species and fluence. Therefore, we do not believe that intermixing is the sole explanation for a barrier layer of constant thickness under a cap which is denuded of pores.

Different cap layer materials have been used to investigate if this denuded layer depends on the type of cap material or not. To examine such effects, different cap layers have been used such as metallic Al and a-Si. Typical results after irradiation with Ge ions are shown in Figs. 11(a)–11(d). Interestingly, the barrier layer thickness does not change from ~8 nm in either case. In addition, since the barrier layer thickness is independent of the type of cap layer used, this reinforces the conclusion that intermixing is not the sole cause of a barrier layer denuded of pores.

Therefore, we have sought a more plausible explanation and propose that the a-Ge layer under the cap that remains denuded of pores is primarily a result of wetting of the cap by a-Ge under ion irradiation. We suggest that the denuded layer is the result of a process of minimisation of surface or interfacial free energy. First, it is well known that, under ion irradiation, a-Si and a-Ge experience the viscous flow.[22–24] Indeed, material flow is one of the mechanisms by which lower density a-Ge/a-Si expands outwards from the surface under ion irradiation, a process driven by stress minimization and mediated by broken bond and defect motion within the amorphous phase.[22] Also, when a-Ge goes porous, the further dramatic expansion of the porous layer is clearly assisted by the viscous flow of the amorphous phase. Hence,

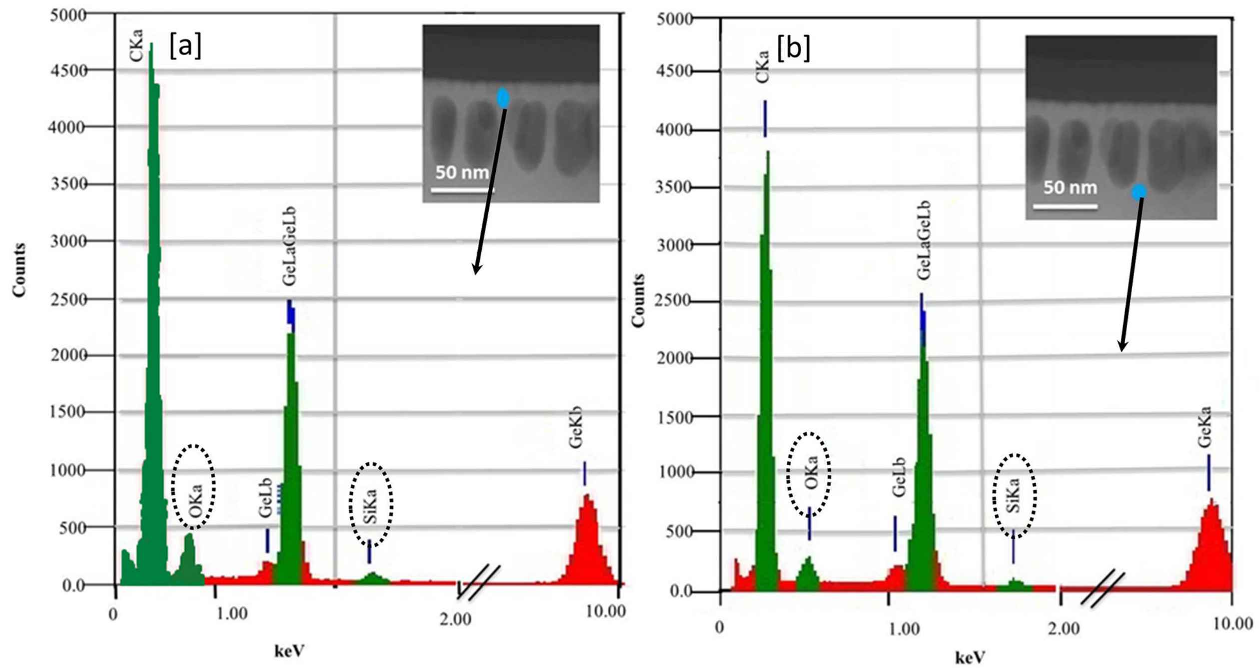

FIG. 10. EDX spectra for 5×10^{15} Ge ions/cm^2 through a 20 nm SiO_2 cap layer. (a) EDX performed in the barrier layer and (b) EDX performed far from the surface.

it might be expected that the presence of a mechanically strong cap may inhibit expansion of a-Ge and thus suppress porosity. Indeed, this is the case at temperatures below room temperature for a SiO_2 cap. However, at higher temperatures lower mechanical strength may cause the cap to flow under ion irradiation, as is the case for SiO_2 and a-Si materials[22,25] and almost certainly true for metallic Al. In such cases, there will now be no impediment to expansion of the underlying a-Ge and development of porosity. We also suggest that interfacial free energy minimisation and wetting processes will control the behaviour of a-Ge material directly under the cap. In this regard, Hu *et al*.[26,27] reported on the case of dewetting of a deposited Pt layer on SiO_2 under irradiation with 800 keV Kr^+ ions. This dewetting phenomenon was attributed to the minimisation of free energy, resulting in the formation of large Pt droplets on the surface with large regions

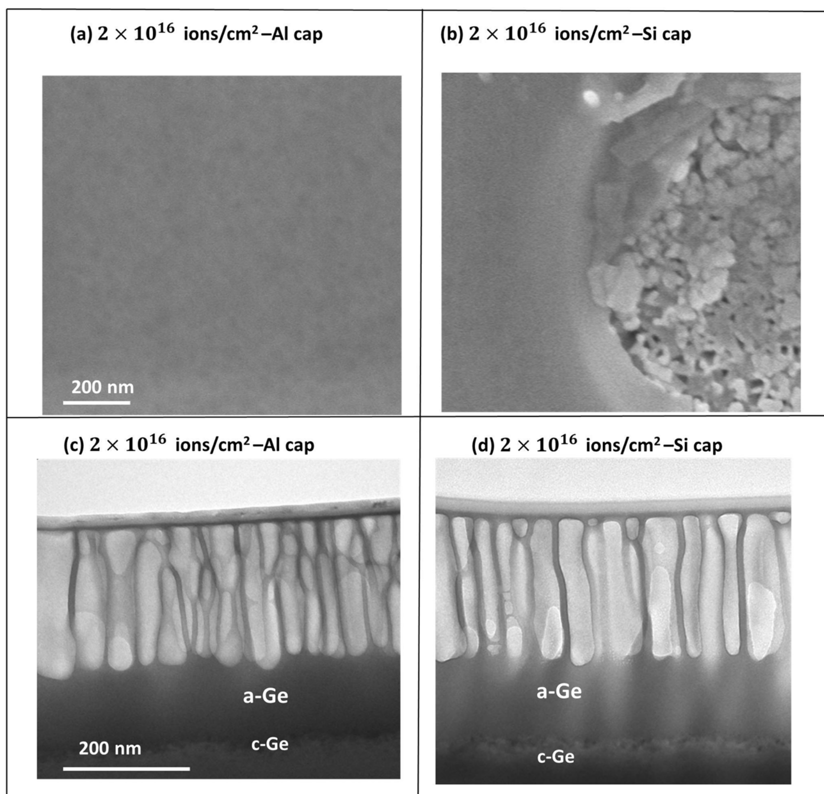

FIG. 11. PVSEM and XTEM images of 2×10^{16} ions/cm^2 140 keV Ge^- ions with different cap layers (40 nm thickness) at RT; (a) and (c) Al cap layer; (b) and (d) a-Si cap layer. The scale bar is the same for all PVSEM and XTEM images.

free of Pt between them. Hence, in our case we suggest that the opposite, wetting phenomenon is operative: stress and viscous flow under irradiation[23,26,27] will drive a-Ge towards the cap layer and wetting and free energy minimisation will control the thickness of a pore-free a-Ge layer under the cap. In addition, once pores form, atomic diffusion at the pore surfaces, and possibly sputtering from the pore walls, may also assist the transport of material towards the cap layer where interfacial minimum free energy considerations (wetting) under the cap will then apply. Consequently, as long as a-Ge wets the cap under the irradiation conditions of this study, the layer denuded of pores will not exhibit any dependence on ion fluence, ion species, thickness and type of the cap layer, and temperature, as is observed experimentally. However, it might be expected that cap materials exist which can cause insufficient wetting (or even dewetting) of a-Ge. Thus, a much wider range of capping materials could be investigated to study the nature of the barrier layer when strong wetting does not occur. We note that the walls of the porous structure, regardless of the presence of a cap, are also denuded of voids and are of a similar thickness to the denuded layer under the cap. However, the walls of pores, once formed, may be sustained by atomic diffusion within the walls and redeposition of material sputtered from the pore bottom, as previously suggested[15] such that the mechanisms that control wall thickness maybe entirely different to that of a-Ge layers under a cap. Clearly, further experiments and calculations will be needed to fully explore this intriguing process of a-Ge flow and wetting of a cap layer.

V. CONCLUSIONS

In this study, we find that there is a significant dependence of pore formation on ion species. Heavier Sn ions promote porosity at LN_2T at a threshold fluence of $>2 \times 10^{16}$ ions/cm^2, whereas Ge ions do not give rise to porosity at LN_2T even at fluences of $> 1 \times 10^{17}$ ions/cm^2. Surprisingly, the presence of a cap layer can eliminate pore formation for both Sn and Ge ions if the irradiation is conducted below both a critical temperature and ion fluence. However, at RT, a cap appears to allow development of a porous layer that is well-ordered and uniform compared to uncapped samples. This is attributed to the cap layer significantly reducing sputtering in the underlying a-Ge layer. Moreover, we have observed a barrier layer denuded of pores of constant 8 nm thickness directly under the cap layer, independent of ion fluence, temperature, ion species, and type of cap. We suggest that this pore-free layer is due to the viscous flow of a-Ge during ion irradiation and wetting of the cap layer as a result of minimization of the interfacial free energy.

ACKNOWLEDGMENTS

We acknowledge the access to the NCRIS and AMMRF infrastructure at the Australian National University including the Heavy Ion Accelerator Capability, the Center for Advanced Microscopy, and the ANFF ACT Node facility. We also thank the Australian Research Council and Dammam University for the financial support.

[1] A. L. Stepanov, V. V. Vorobev, Y. N. Osin, M. A. Ermakov, V. F. Valeev, and V. I. Nuzhdin, Sci. J. Microelectron. **4**(3), 11–17 (2014).
[2] T. T. Tran, H. S. Alkhaldi, H. H. Gandhi, D. Pastor, L. Q. Huston, J. Wong-Leung, M. J. Aziz, and J. S. Williams, Appl. Phys. Lett. **109**(8), 082106 (2016).
[3] M. R. Baklanov and K. Maex, Philos. Trans. R. Soc. London, Ser. A **364**(1838), 201–215 (2006).
[4] I. H. Wilson, J. Appl. Phys. **53**(3), 1698 (1982).
[5] B. Stritzker, R. G. Elliman, and J. Zou, Nucl. Instrum. Methods Phys. Res., Sect. B. **175–177**, 193–196 (2001).
[6] L. Romano, G. Impellizzeri, L. Bosco, F. Ruffino, M. Miritello, and M. G. Grimaldi, J. Appl. Phys. **111**(11), 113515 (2012).
[7] A. Belafhaili, L. Laânab, F. Cristiano, N. Cherkashin, and A. Claverie, Mater. Sci. Semicond. Process **16**(6), 1655–1658 (2013).
[8] B. R. Appleton, O. W. Holland, D. B. Poker, J. Narayan, and D. Fathy, Nucl. Instrum. Methods Phys. Res., Sect. B **7–8** (MAR), 639–644 (1985).
[9] B. L. Darby, B. R. Yates, N. G. Rudawski, K. S. Jones, A. Kontos, and R. G. Elliman, Thin Solid Films **519**(18), 5962–5965 (2011).
[10] N. G. Rudawski, B. L. Darby, B. R. Yates, K. S. Jones, R. G. Elliman, and A. A. Volinsky, Appl. Phys. Lett. **100**(8), 083111 (2012).
[11] M. E. Davis, Nature **417**(6891), 813–821 (2002).
[12] J.-H. Lee and J. C. Grossman, Appl. Phys. Lett. **95**(1), 013106 (2009).
[13] G. Q. Lu and X. S. Zhao, *Nanoporous Materials Science and Engineering* (Imperial College Press, London, 2004).
[14] O. W. Holland, B. R. Appleton, and J. Narayan, J. Appl. Phys. **54**(5), 2295 (1983).
[15] H. S. Alkhaldi, F. Kremer, T. Bierschenk, J. L. Hansen, A. Nylandsted-Larsen, J. S. Williams, and M. C. Ridgway, J. Appl. Phys. **119**(9), 094303 (2016).
[16] E. Bruno, G. G. Scapellato, G. Bisognin, E. Carria, L. Romano, A. Carnera, and F. Priolo, J. Appl. Phys. **108**(12), 124902 (2010).
[17] T. Janssens, C. Huyghebaert, D. Vanhaeren, G. Winderickx, A. Satta, M. Meuris, and W. Vandervorst, J. Vac. Sci. Technol., B **24**(1), 510 (2006).
[18] B. L. Darby, Ph.D. thesis, University of Florida, 2012.
[19] B. Yates, B. Darby, R. Elliman, and K. Jones, Appl. Phys. Lett. **101**(13), 131907 (2012).
[20] J. F. Ziegler, J. P. Biersack, and U. Littmark, *The Stopping and Range of Ions in Solids* (Pergamon, New York, 1984).
[21] L. Romano, G. Impellizzeri, M. V. Tomasello, F. Giannazzo, C. Spinella, and M. G. Grimaldi, J. Appl. Phys. **107**(8), 084314 (2010).
[22] C. A. Volkert, J. Appl. Phys. **70**(7), 3521–3527 (1991).
[23] A. Witvrouw and F. Spaepen, J. Appl. Phys. **74**(12), 7154–7161 (1993).
[24] S. Mayr and R. Averback, Phys. Rev. B: Condens. Matter **71**(13), 134102 (2005).
[25] E. Snoeks, A. Polman, and C. Volkert, Appl. Phys. Lett. **65**(19), 2487–2489 (1994).
[26] X. Hu, D. G. Cahill, and R. S. Averback, J. Appl. Phys. **89**(12), 7777–7783 (2001).
[27] X. Hu, D. G. Cahill, and R. S. Averback, Appl. Phys. Lett. **76**(22), 3215 (2000).